

~~CONFIDENTIAL~~Copy  
RM L53G14a

NACA RM L53G14a

~~53-36-12~~NACA

0144387

TECH LIBRARY KAFB, NM

## RESEARCH MEMORANDUM

WIND-TUNNEL INVESTIGATION OF THE  
AERODYNAMIC CHARACTERISTICS IN PITCH AND SIDESLIP AT HIGH  
SUBSONIC SPEEDS OF A WING-FUSELAGE COMBINATION HAVING A  
TRIANGULAR WING OF ASPECT RATIO 4

By Paul G. Fournier

Langley Aeronautical Laboratory  
Langley Field, Va.

This material contains information affecting the national defense of the United States within the meaning of the espionage laws, Title 18, U.S.C., Secs. 793 and 794, the transmission or revelation of which in any manner to an unauthorized person is prohibited by law.

NATIONAL ADVISORY COMMITTEE  
FOR AERONAUTICS

WASHINGTON

August 28, 1953

~~RECEIPT SIGNATURE  
REQUIRED~~~~CONFIDENTIAL~~~~MADE 2228~~

6777L

Classification cancelled (or changed to) Unclassified

By Authority of NASA TOL Rb Announcement #13/  
(OFFICER AUTHORIZED TO CHANGE)

By .....

8 Aug 56

JK

GRADE OF OFFICER MAKING CHANGE

5 Apr 67  
DATE



## NATIONAL ADVISORY COMMITTEE FOR AERONAUTICS

## RESEARCH MEMORANDUM

WIND-TUNNEL INVESTIGATION OF THE  
AERODYNAMIC CHARACTERISTICS IN PITCH AND SIDESLIP AT HIGH  
SUBSONIC SPEEDS OF A WING-FUSELAGE COMBINATION HAVING A  
TRIANGULAR WING OF ASPECT RATIO 4

By Paul G. Fournier

## SUMMARY

The results presented in the present paper are part of a program conducted to investigate the effect of wing plan form on the aerodynamic characteristics in pitch, in sideslip, and during steady roll. This paper presents the aerodynamic characteristics in pitch and sideslip at high subsonic speeds of a wing-fuselage combination having a triangular wing of aspect ratio 4, a leading-edge sweep angle of  $45^\circ$ , and with an NACA 65A006 airfoil section parallel to the plane of symmetry. The range of Mach number was from 0.40 to 0.95 at a range of Reynolds number from  $2.4 \times 10^6$  to  $3.9 \times 10^6$ .

The results indicate that the effective-dihedral parameter  $C_{l\beta C_L}$  determined at low lift coefficients for the wing-fuselage combination is considerably higher than would be expected from available methods - particularly in the range of Mach number from 0.75 to 0.92.

The wing-fuselage combination was longitudinally unstable at lift coefficients from approximately 0.50 to 0.70 and at Mach numbers from 0.40 to 0.80. At Mach numbers above 0.80, the high-lift stability appeared to improve.

## INTRODUCTION

A systematic research program is being conducted in the Langley high-speed 7- by 10-foot wind tunnel to determine the aerodynamic characteristics of various model configurations in pitch, in sideslip, and during steady roll up to a Mach number of about 0.95.

The data presented in this paper were obtained from tests of a wing-fuselage combination having a triangular wing of aspect ratio 4 with leading-edge sweep angle of  $45^\circ$  and an NACA 65A006 airfoil section parallel to the plane of symmetry. The pitch and sideslip data for the

~~CONFIDENTIAL~~

11-000-2228

fuselage alone are presented in references 1 and 2, respectively. The range of Reynolds number for the sting-supported model tested varied from  $2.4 \times 10^6$  to  $3.9 \times 10^6$ . In order to expedite the issuance of the results, only a limited analysis of some of the more significant characteristics is presented.

#### COEFFICIENTS AND SYMBOLS

The stability system of axes used for the presentation of the data together with an indication of the positive forces, moments, and angles are presented in figure 1. All moments are referred to the quarter-chord point of the wing mean aerodynamic chord.

$C_L$	lift coefficient, Lift/qS
$C_D$	drag coefficient, Drag/qS
$C_m$	pitching-moment coefficient, Pitching moment/qS $\bar{c}$
$C_l$	rolling-moment coefficient, Rolling moment/qSb
$C_n$	yawing-moment coefficient, Yawing moment/qSb
$C_y$	lateral-force coefficient, Lateral force/qS
$\Delta C_D$	drag due to lift, $C_D - C_{D_{C_L=0}}$
$\Delta C_{D_{bp}}$	base pressure-drag coefficient
$C_{D_{C_L=0}}$	drag at zero lift
$L/D$	lift-drag ratio, $C_L/C_D$
$q$	dynamic pressure, $\rho V^2/2$ , lb/sq ft
$\rho$	mass density of air, slugs/cu ft
$V$	free-stream velocity, fps
$M$	Mach number

- R Reynolds number,  $\rho V \bar{c} / \mu$
- $\mu$  absolute viscosity of air, slugs/ft-sec
- A aspect ratio,  $b^2/S$
- S wing area, sq ft
- b span, ft
- c local chord, ft
- $\bar{c}$  mean aerodynamic chord,  $\frac{2}{S} \int_0^{b/2} c^2 dy$ , ft
- y spanwise station, ft
- $\alpha$  angle of attack, deg
- $\beta$  angle of sideslip, deg
- $C_{L\alpha}$  lift-curve slope per deg,  $\partial C_L / \partial \alpha$
- $C_{l\beta} = \frac{\partial C_l}{\partial \beta}$  per deg
- $C_{n\beta} = \frac{\partial C_n}{\partial \beta}$  per deg
- $C_{Y\beta} = \frac{\partial C_Y}{\partial \beta}$  per deg
- $C_{l\beta C_L} = \frac{\partial C_{l\beta}}{\partial C_L}$  per deg

## MODEL AND APPARATUS

The wing-fuselage combination tested is shown in figure 2. The wing, made of aluminum alloy, had an NACA 65A006 airfoil section parallel to the plane of symmetry and was attached in a midwing position to the aluminum fuselage. The ordinates of the fuselage are presented in reference 1. The wing aspect ratio is 4 and the leading-edge sweep angle is  $45^\circ$ .

The model was tested on the sting-type support system shown in figures 3 and 4. With this support system the model can be remotely operated through a  $28^\circ$  angle range in the plane of the vertical strut. By means of couplings in the sting, the model can be rolled through  $90^\circ$  so that either angle of attack (fig. 3) or angle of sideslip (fig. 4) can be the remotely controlled variable. With the model in a horizontal position (fig. 3), couplings can be used to support the model at angles of sideslip of approximately  $-4^\circ$  and  $4^\circ$  while the model is tested through the range of angle of attack. The data were obtained by use of an internally mounted electrical strain-gage balance.

### TEST AND CORRECTIONS

The tests were conducted in the Langley high-speed 7- by 10-foot wind tunnel through a range of Mach number from 0.40 to 0.95. The size of the model caused the tunnel to choke at a corrected Mach number of about 0.96. The blocking corrections which were applied to the data were determined by the velocity-ratio method of reference 3.

Jet-boundary corrections, which were applied to angle of attack, lift, and drag, were calculated by the method of reference 4. The corrections to pitching moment, lateral force, yawing moment, and rolling moment were considered negligible.

Sting-support tares were determined, but were found to be negligible for a wing-fuselage combination except for drag. The drag tare results from the influence of the sting on the external model pressure - particularly near the rearward end. This tare value amounted to a drag-coefficient increment of about 0.002 throughout the test ranges of angle of attack and Mach number and should be added to the drag data presented. The correction has not been applied as some uncertainty exists regarding its exact magnitude and also because the correction was obtained after the results of some investigations (for example, ref. 1) which are related to the results of the present investigation had already been published. The angle of attack and angle of sideslip have been corrected for the deflection of the sting-support system and balance under load.

The drag data have been corrected to correspond to a pressure at the base of the fuselage equal to free-stream static pressure. For this correction, the base pressure was determined by measuring the pressure

inside the fuselage at a point about 9 inches forward of the base. The following corrections were added to the measured drag coefficients:

M	$C_{D_{bp}}$
0.40	0.0022
.60	.0022
.80	.0027
.90	.0032
.95	.0033

No corrections were made for the effects of aeroelastic distortion. Experience with other related plan forms indicate that these effects would be small. The variation with Mach number of the mean test Reynolds number based on the wing mean aerodynamic chord is presented in figure 5.

## RESULTS AND DISCUSSION

The results of the present investigation are presented in the following figures:

	<u>Figures</u>
Basic data:	
Longitudinal . . . . .	6
Lateral . . . . .	7
Summary plots:	
Effects of Mach number . . . . .	8
Drag due to lift . . . . .	9
Effective dihedral parameter . . . . .	10

The basic longitudinal and lateral data for the fuselage alone were previously presented in references 1 and 2, respectively.

The basic pitching-moment characteristics (fig. 6(b)) indicate longitudinal instability of the wing-fuselage combination at a range of Mach number from 0.40 to 0.80 and at a range of lift coefficient from approximately 0.50 to 0.70. The rearward shift in low-lift aerodynamic-center position which begins at about 0.80 Mach number seems to be accompanied by a somewhat improved high-lift stability.

The basic data of figure 7(a) also show that at high lift coefficients the values of  $C_{l_{\beta}}$  are considerably larger at high subsonic Mach numbers than at low speeds. The effective dihedral parameter  $C_{l_{\beta}C_L}$

determined at low lift coefficients through the range of Mach number is presented in figure 10. The experimental values are compared with the theoretical values computed by the method of reference 5 and corrected for the effects of Mach number by the method of reference 6. The experimental values are considerably higher than the estimated values, particularly in the range of Mach number from 0.75 to 0.92. For the wing tested,  $C_{l\beta_{CL}}$  exhibited a rapid reduction in magnitude with Mach number above the force-break Mach number.

Some of the more important stability derivatives are presented in figure 8. The experimental values of  $C_{L\alpha}$  show fair agreement with the wing-alone values calculated by the method of reference 7. The experimental maximum lift-drag ratio is compared with two theoretical curves.

The upper curve (ref. 8),  $\frac{1}{2} \sqrt{\frac{\pi A}{C_{D_{CL=0}}}}$ , was obtained from the experimental drag at zero lift  $C_{D_{CL=0}}$  and the induced drag factor for potential flow for an elliptical loading  $1/\pi A$  and represents the condition of the resultant force normal to the local relative wind (full leading-edge suction). The lower curve,  $\frac{1}{2} \sqrt{\frac{57.3 C_{L\alpha}}{C_{D_{CL=0}}}}$ , was obtained from the experimental drag at zero lift  $C_{D_{CL=0}}$  and the experimental lift-curve slope  $C_{L\alpha}$  and represents the condition of the resultant force due to angle of attack normal to the wing chord.

For the present wing, the experimental values of  $(L/D)_{max}$  lie between the two theoretical curves up to a Mach number of about 0.85, then approach the curve which is based on the assumption that the resultant force is normal to the wing chord. The decrease in experimental values of  $(L/D)_{max}$  above a Mach number of 0.85 is due to a higher drag due to lift at the higher Mach numbers (fig. 9).

#### CONCLUSIONS

The results of the present investigation of the aerodynamic characteristics in pitch and sideslip at high subsonic speeds of a wing-fuselage combination having a triangular wing of aspect ratio 4, a leading-edge sweep angle of  $45^\circ$ , and with an NACA 65A006 airfoil section parallel to the plane of symmetry indicate the following conclusions:

1. The effective-dihedral parameter  $C_{l\beta_{CL}}$  determined at low lift coefficients was found to be considerably higher than would be expected from available methods - particularly in the range of Mach number from 0.75 to 0.92.

2. The wing-fuselage combination was longitudinally unstable at lift coefficients from approximately 0.50 to 0.70 and at Mach numbers from 0.40 to 0.80. At higher Mach numbers the high-lift stability appeared to improve.

Langley Aeronautical Laboratory,  
National Advisory Committee for Aeronautics,  
Langley Field, Va., July 1, 1953.

~~CONFIDENTIAL~~

## REFERENCES

1. Kuhn, Richard E., and Wiggins, James W.: Wind-Tunnel Investigation of the Aerodynamic Characteristics in Pitch of Wing-Fuselage Combinations at High Subsonic Speeds. Aspect-Ratio Series. NACA RM L52A29, 1952.
2. Kuhn, Richard E., and Fournier, Paul G.: Wind-Tunnel Investigation of the Static Lateral Stability Characteristics of Wing-Fuselage Combinations at High Subsonic Speeds - Sweep Series. NACA RM L52G11a, 1952.
3. Hensel, Rudolph W.: Rectangular-Wind-Tunnel Blocking Corrections Using the Velocity-Ratio Method. NACA TN 2372, 1951.
4. Gillis, Clarence L., Polhamus, Edward C., and Gray, Joseph L., Jr.: Charts for Determining Jet-Boundary Corrections for Complete Models in 7- by 10-Foot Closed Rectangular Wind Tunnels. NACA WR L-123, 1945. (Formerly NACA ARR L5G31.)
5. Toll, Thomas A., and Queijo, M. J.: Approximate Relations and Charts for Low-Speed Stability Derivatives of Swept Wings. NACA TN 1581, 1948.
6. Fisher, Lewis R.: Approximate Corrections for the Effects of Compressibility on the Subsonic Stability Derivatives of Swept Wings. NACA TN 1854, 1949.
7. DeYoung, John: Theoretical Additional Span Loading Characteristics of Wings With Arbitrary Sweep, Aspect Ratio, and Taper Ratio. NACA TN 1491, 1947.
8. Jones, Robert T.: Estimated Lift-Drag Ratios at Supersonic Speed. NACA TN 1350, 1947.

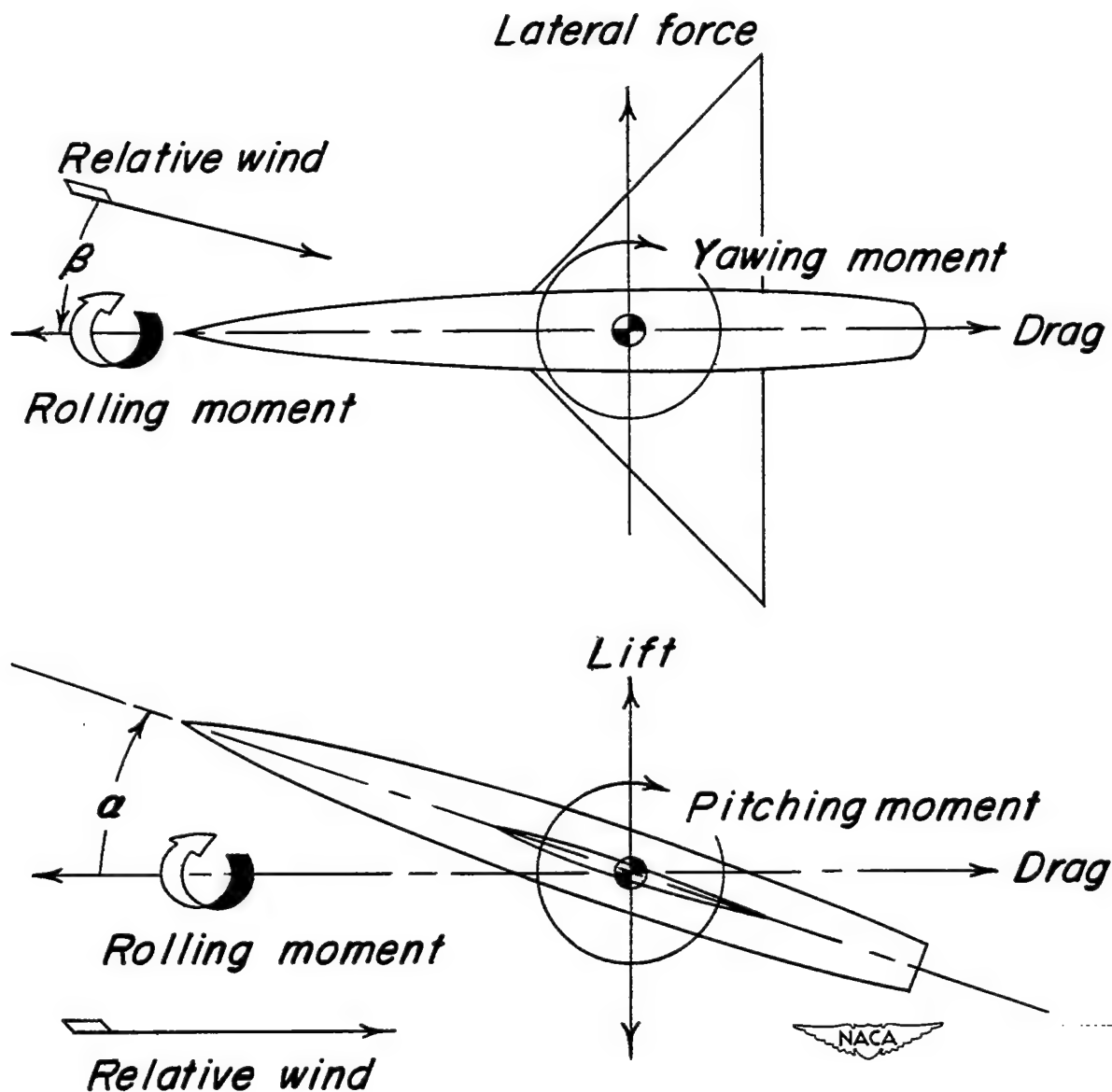


Figure 1.- Stability system of axes showing positive direction of forces, moments, and angles.

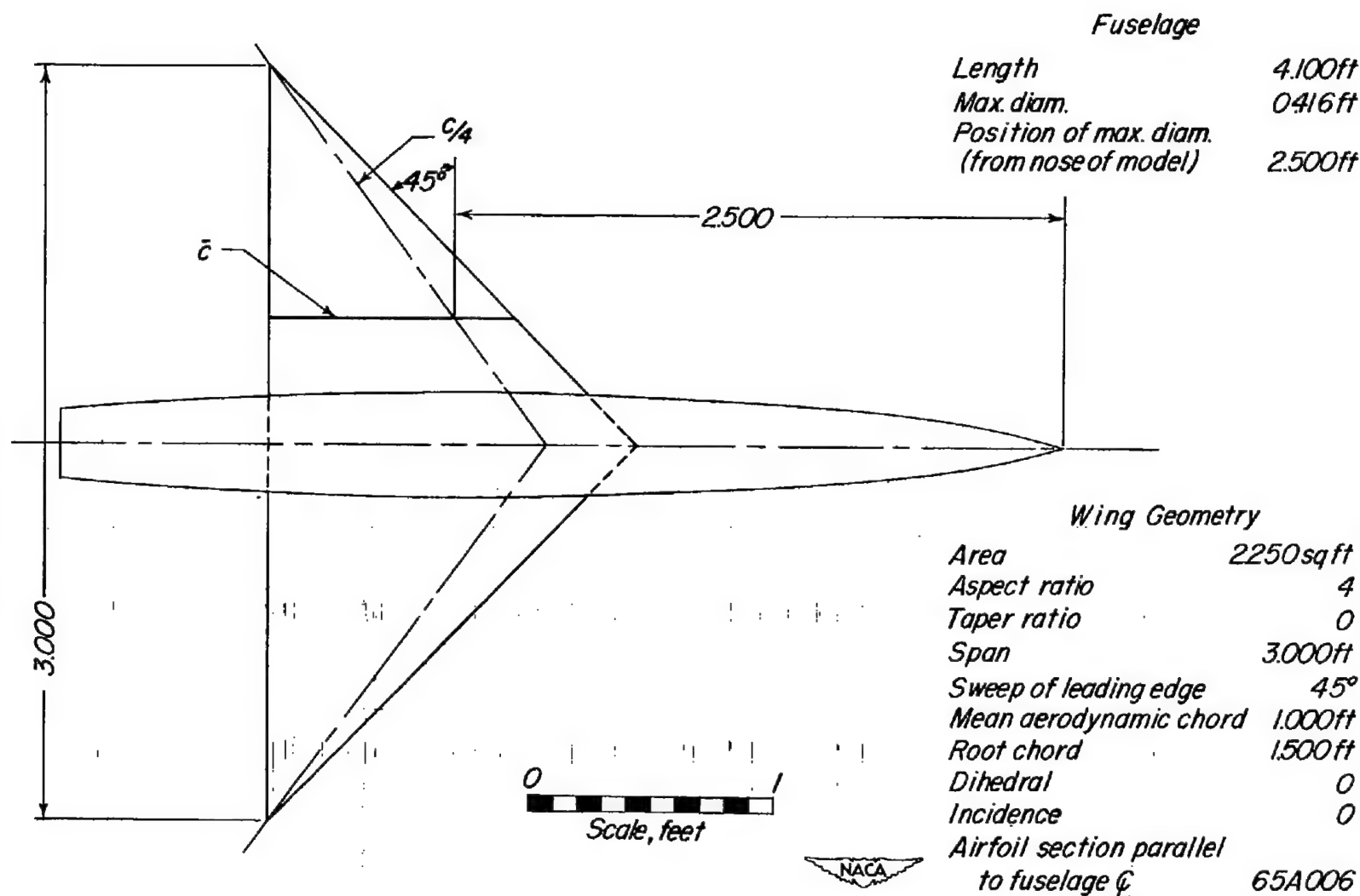
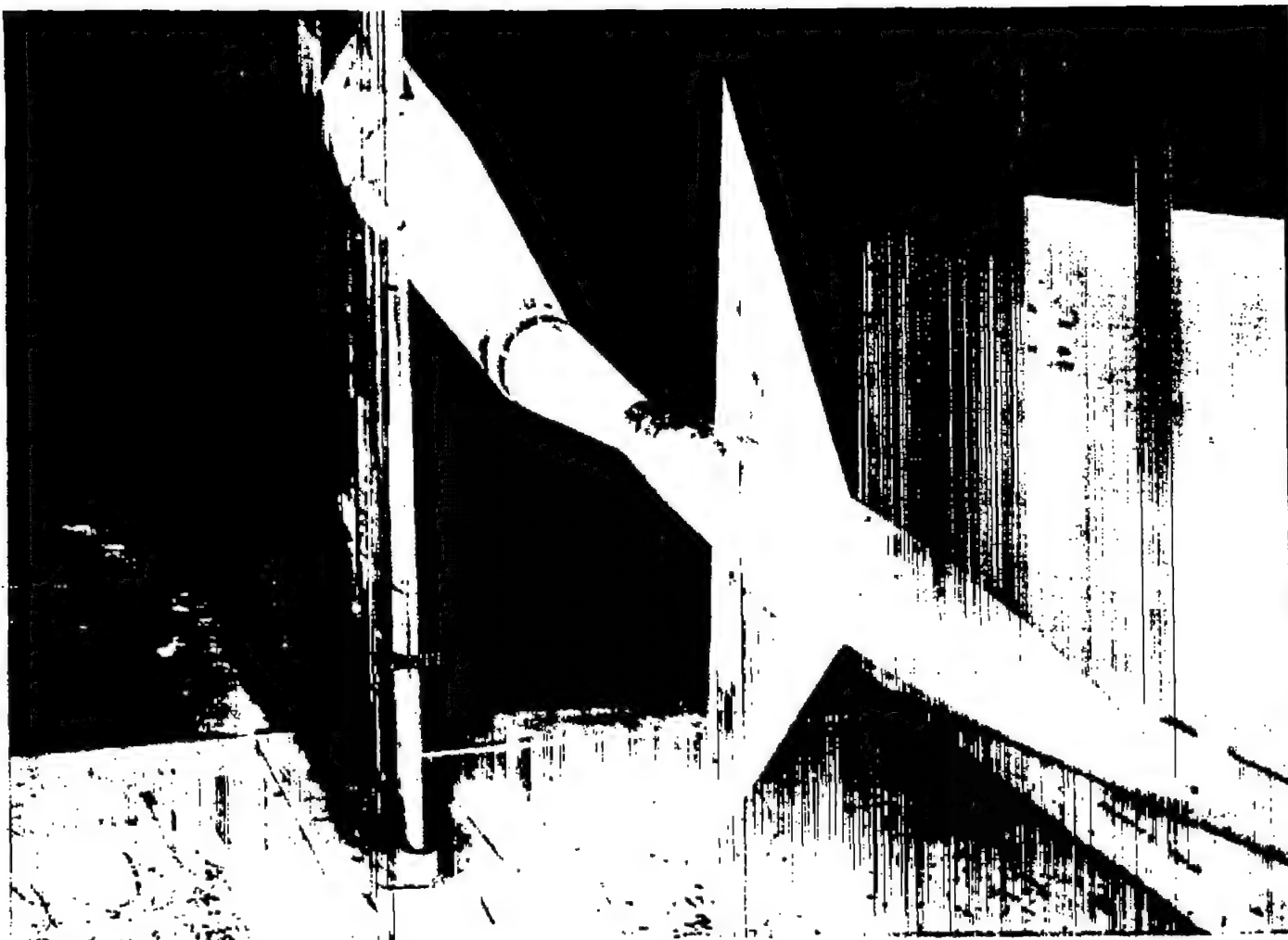


Figure 2.- Drawing of triangular wing of aspect ratio 4.



L-79562

Figure 3.- Model installed on sting support system for tests of variable angles of attack shown at  $0^\circ$  angle of sideslip.



L-79561

Figure 4.- Model installed for tests of variable angles of sideslip shown  
at  $0^\circ$  angle of attack.

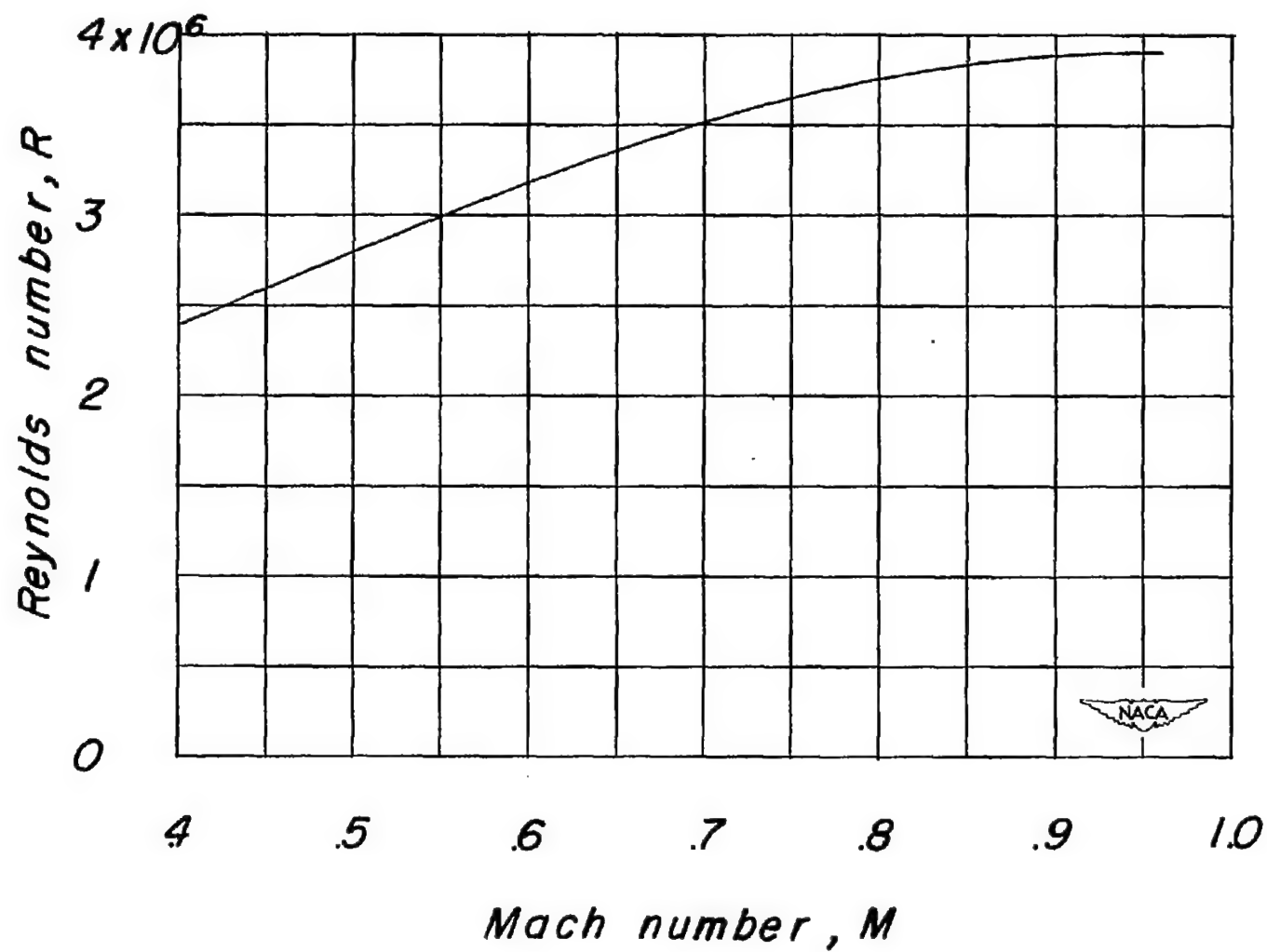
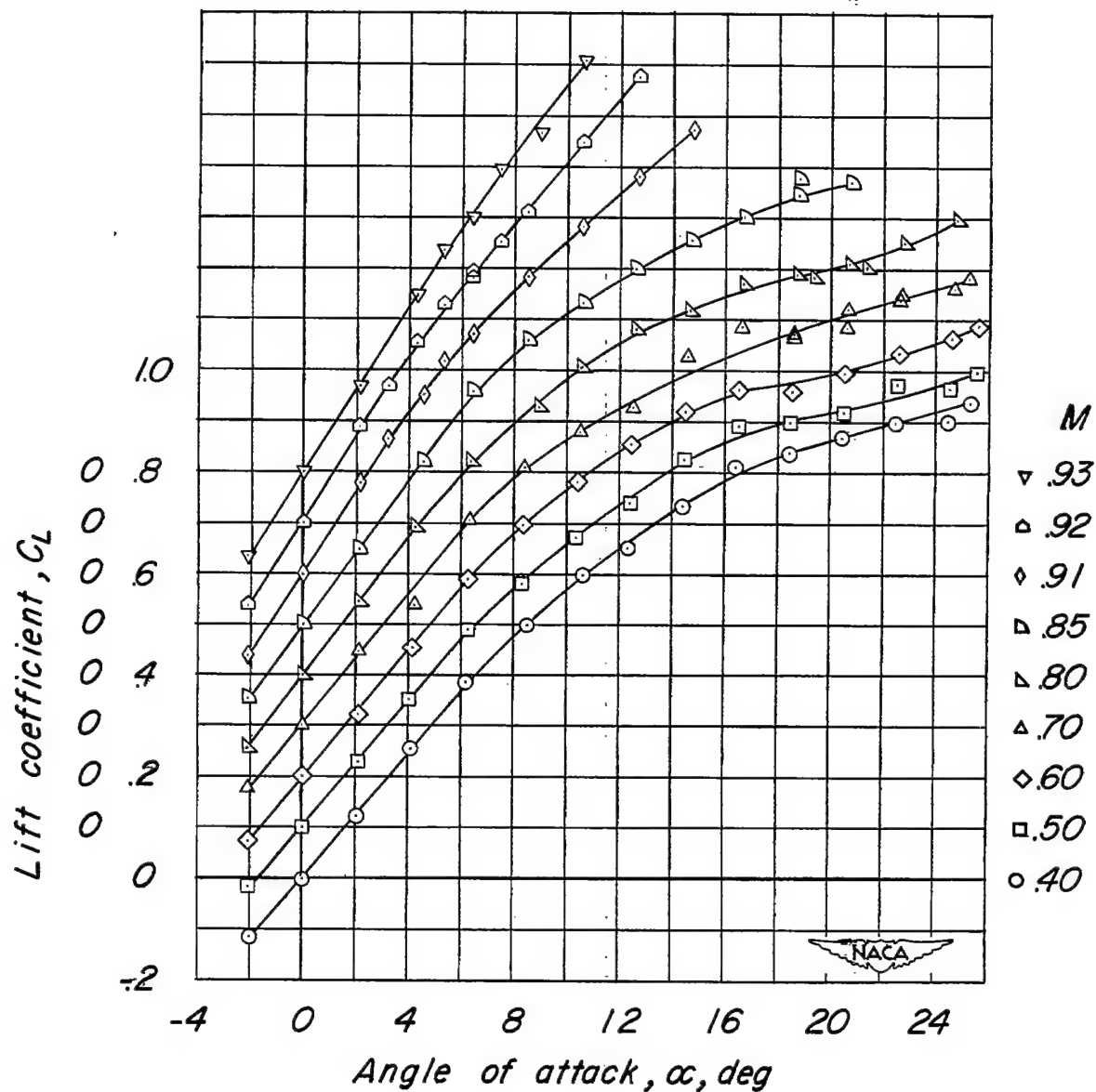
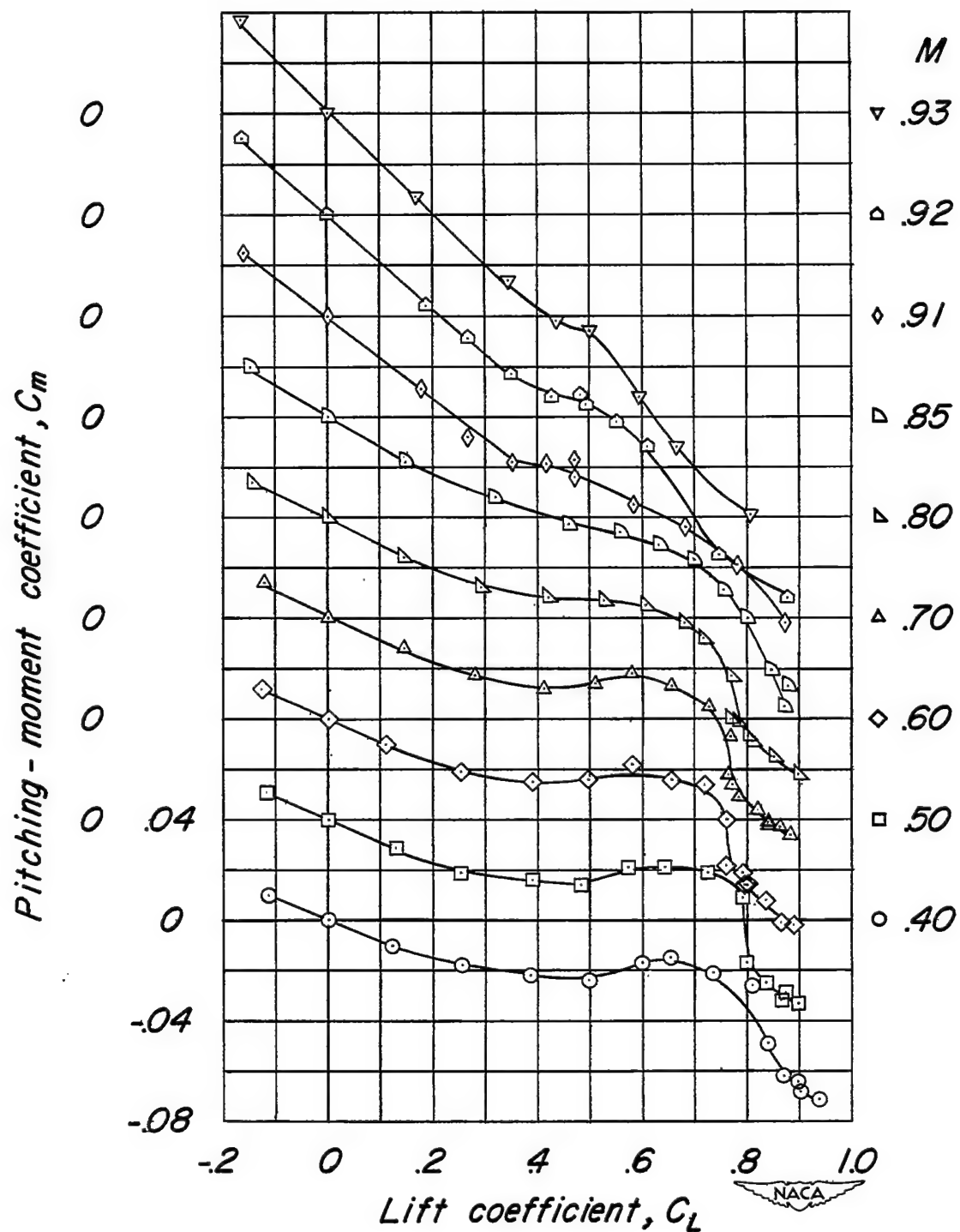


Figure 5.- Variation of mean Reynolds number with test Mach number based on wing mean aerodynamic chord.



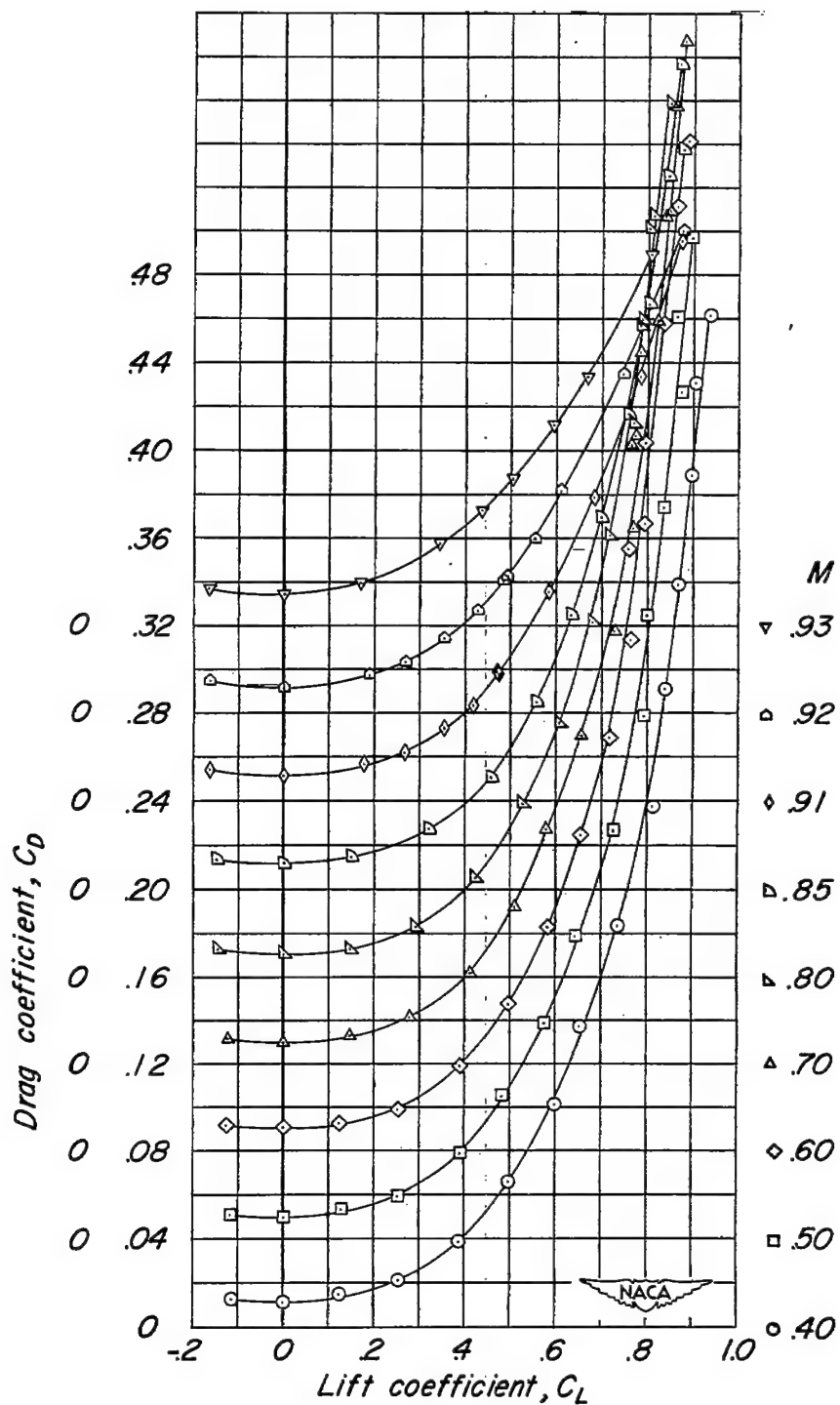
(a) Lift.

Figure 6.- Longitudinal stability characteristics of a wing-fuselage combination having a triangular wing of aspect ratio 4. Data are not corrected for aeroelastic distortion.



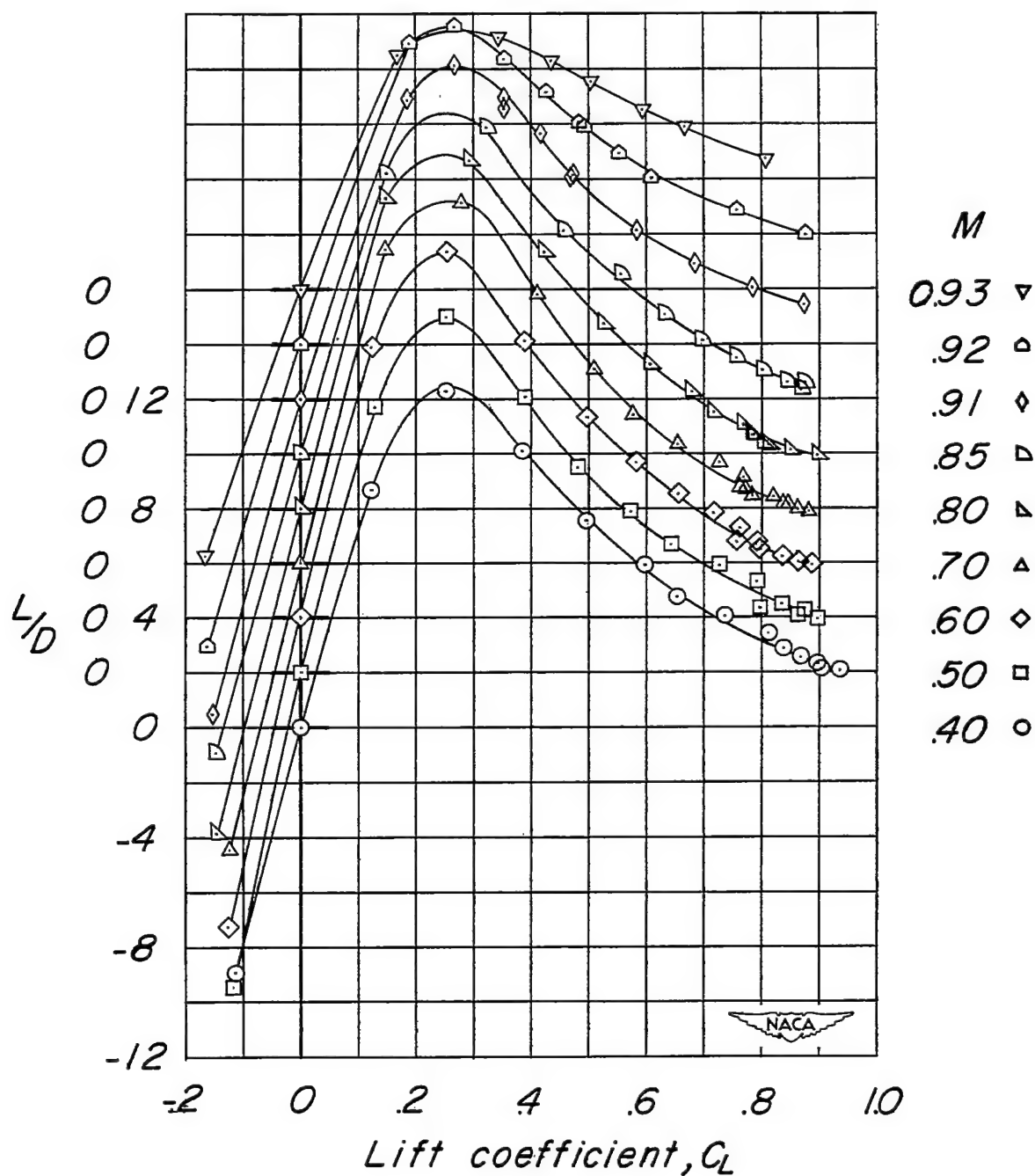
(b) Pitching-moment characteristics.

Figure 6.- Continued.



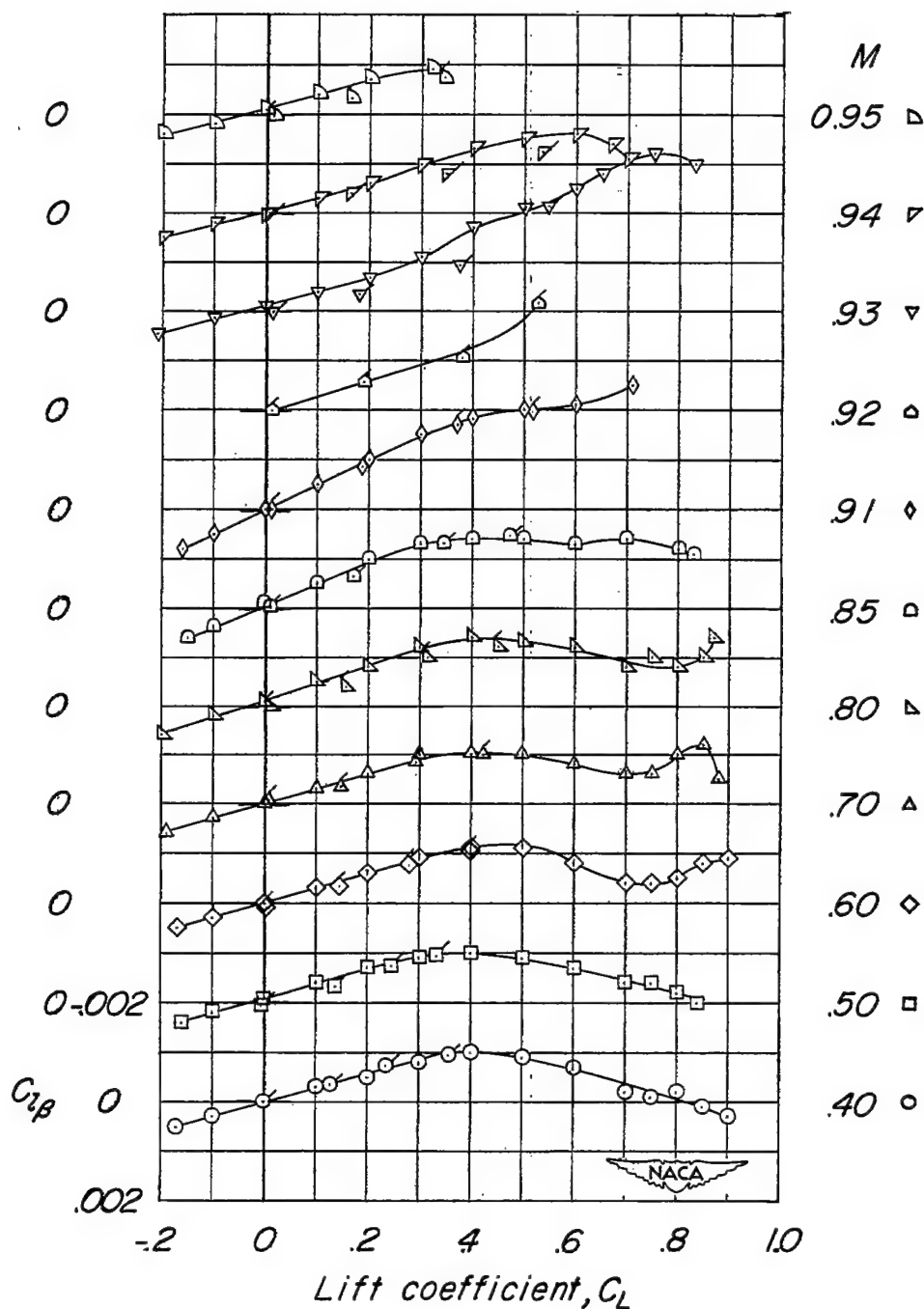
(c) Drag. Drag data are corrected for free-stream static pressure at fuselage base, but not for sting-interference tare.

Figure 6.- Continued.



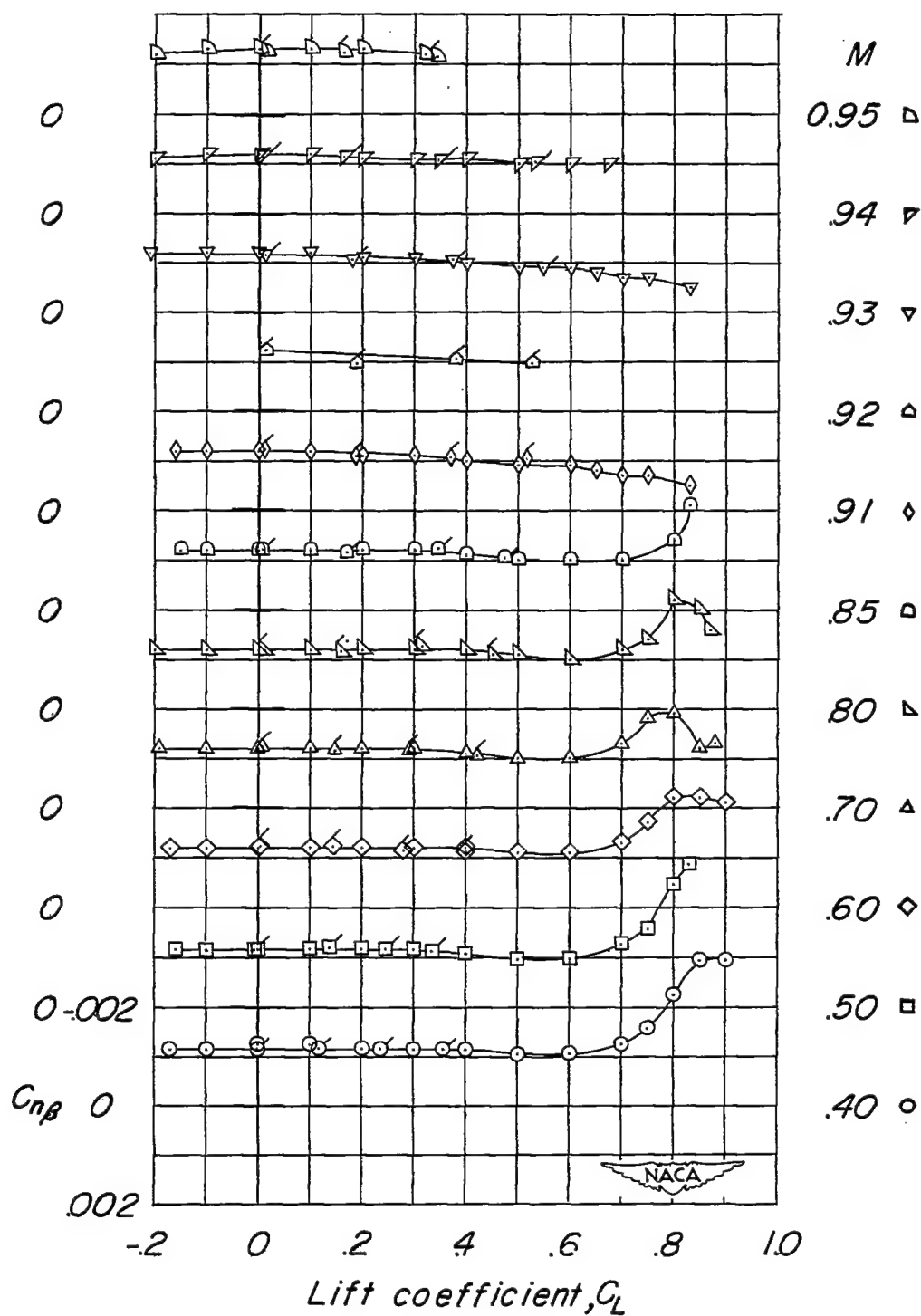
(d) Lift-drag ratios. Drag data are corrected for free-stream static pressure at fuselage base, but not for sting-interference tare.

Figure 6.- Concluded.



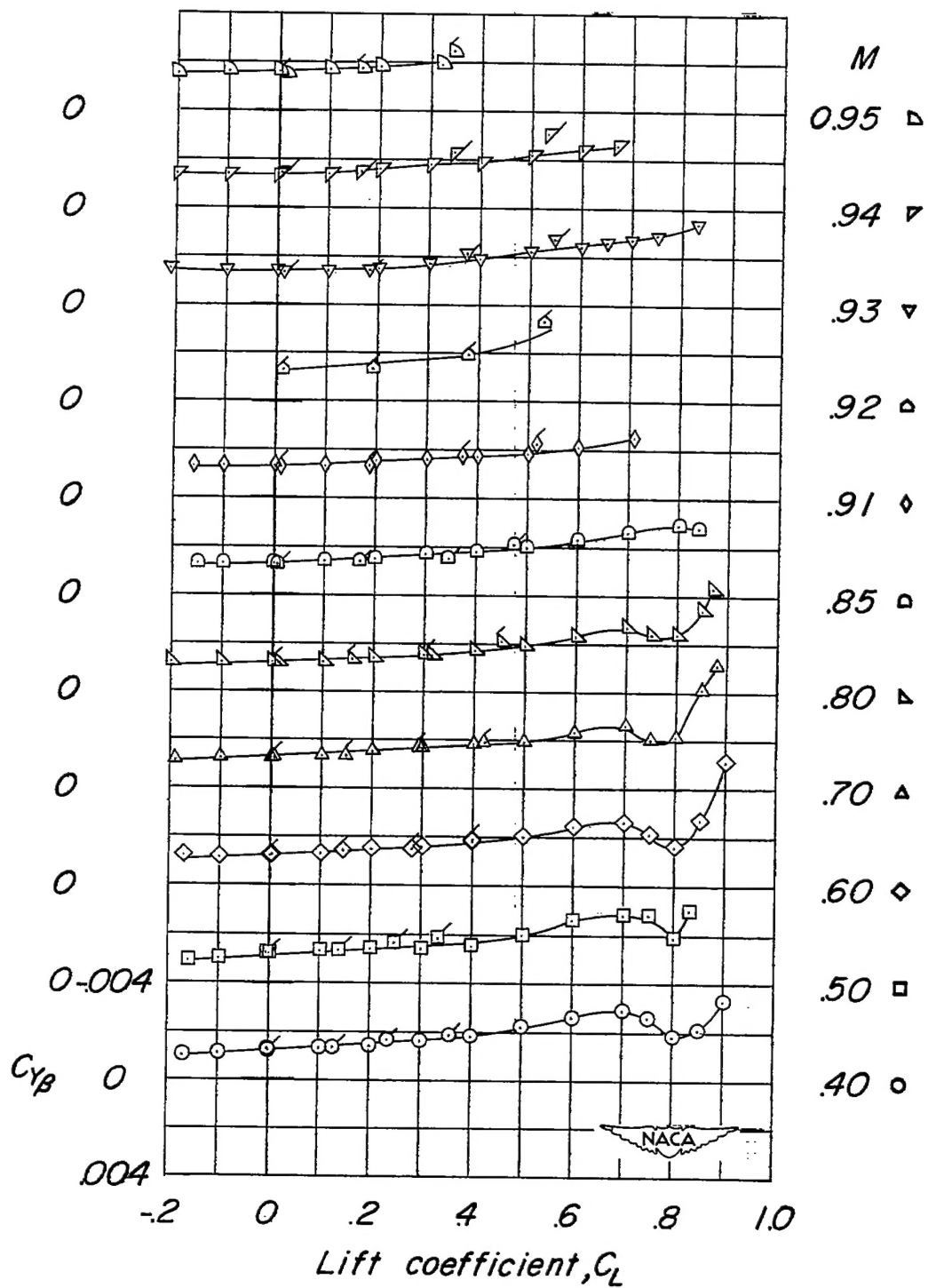
(a) Rolling moment due to sideslip.

Figure 7.- Lateral stability characteristics of a wing-fuselage combination having a triangular wing of aspect ratio 4. Data are not corrected for aeroelastic distortion. Flagged symbols represent tests in which angle of sideslip was varied.



(b) Yawing moment due to sideslip.

Figure 7.- Continued.



(c) Lateral force due to sideslip.

Figure 7.- Concluded.

~~CONFIDENTIAL~~

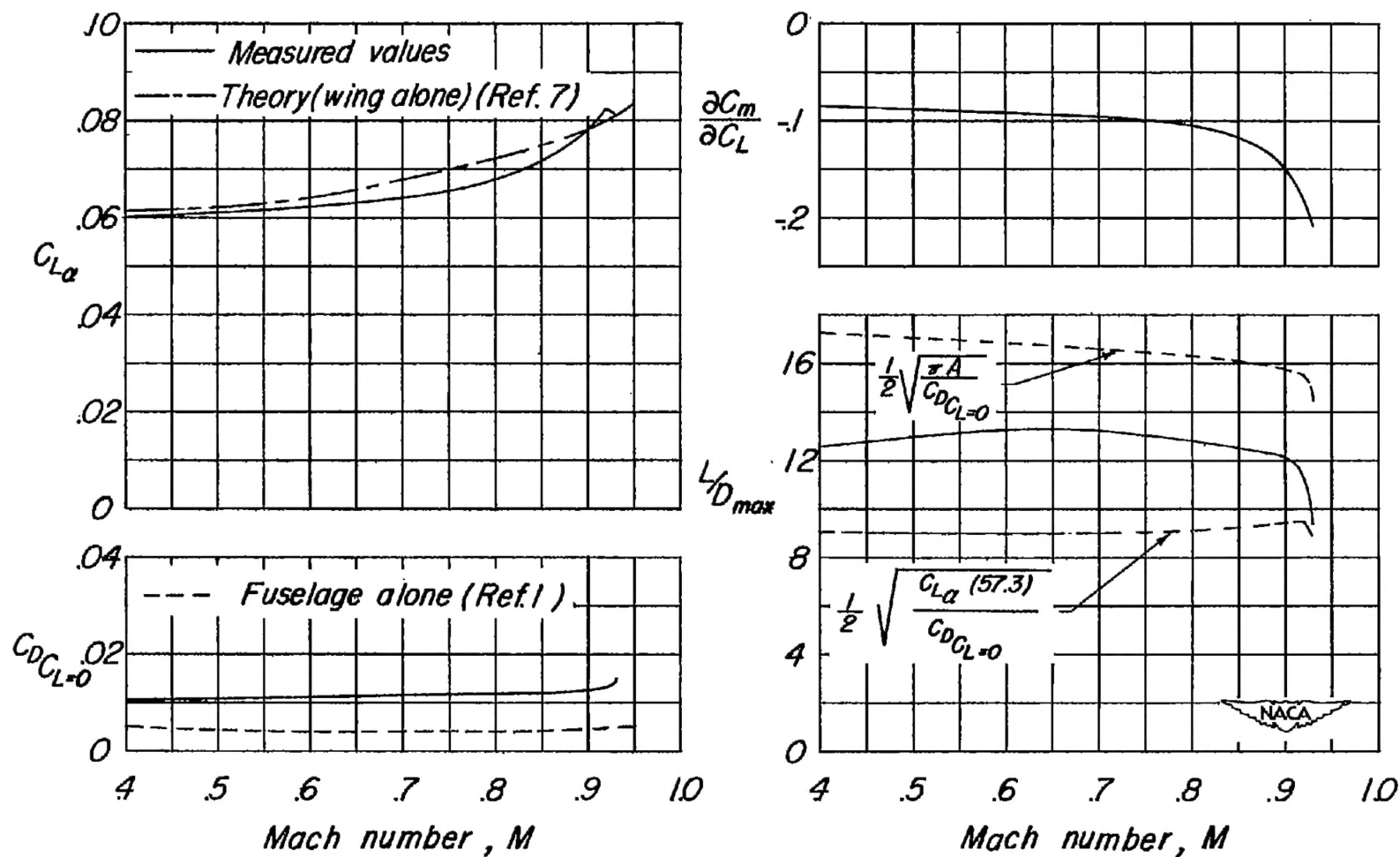


Figure 8.- Summary of effects of Mach number on aerodynamic characteristics of a wing-fuselage combination having a triangular wing of aspect ratio 4. Drag data are corrected for free-stream static pressure at fuselage base, but not for sting-interference tare.

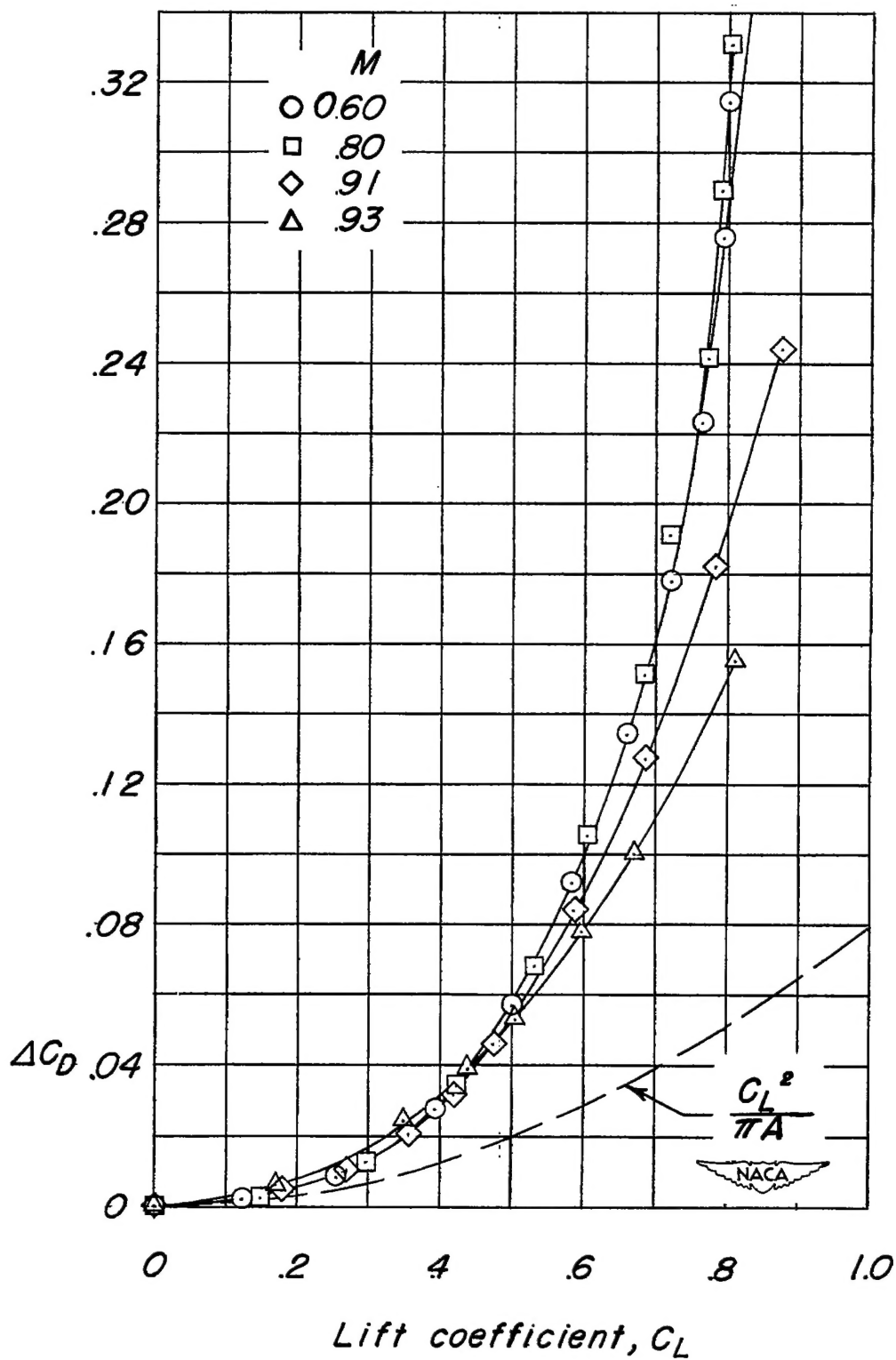


Figure 9.- Drag due to lift at several Mach numbers for a wing-fuselage combination having a triangular wing of aspect ratio 4.

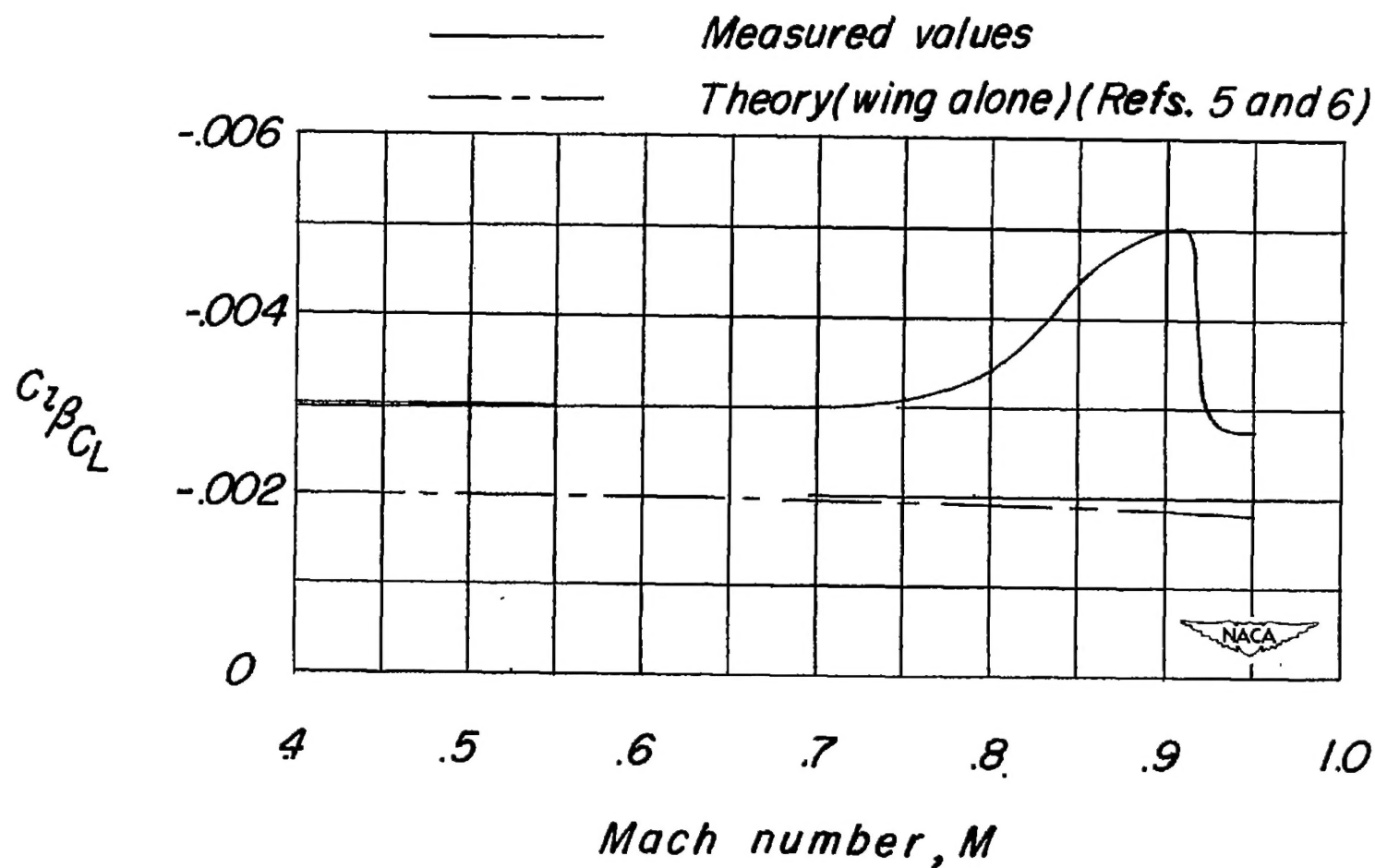


Figure 10.- Effective-dihedral parameter of a wing-fuselage combination having a triangular wing of aspect ratio 4.  $\alpha \approx 0^\circ$ .